

## Robustness of noise induced resonances

J. Escalona<sup>a</sup> and P. Parmananda<sup>a,b</sup>

<sup>a</sup>*Facultad de Ciencias, Universidad Autónoma del Estado de Morelos,  
Avenida Universidad 1001, Colonia Chamilpa 62209, Cuernavaca, Morelos, México.*

<sup>b</sup>*Department of Physics, Indian Institute of Technology Bombay,  
Powai, Mumbai 400076, India.*

Recibido el 10 de diciembre de 2008; aceptado el 20 de enero de 2009

In order to confirm the emergence of resonances in the presence of non-stationary noise, an excitable FitzHugh-Nagumo (FN) system is subjected to stochastic forcing both in the absence and in the presence of sub-threshold signals. This non-stationarity of noise is mimicked by varying the noise sequence (seed) for each amplitude of the superimposed noise while preserving their statistical properties. Our numerical computations indicate that noise induced resonances for this non-stationarity stochastic forcing become less conclusive for complex subthreshold signals.

*Keywords:* Stochastic resonance; excitable system.

Para confirmar la aparición de resonancias en la presencia de ruido no estacionario, utilizamos un sistema tipo FitzHugh-Nagumo (FN) sujeto a fuerzas estocásticas tanto en ausencia, así como en presencia de señales subumbrales. Simulamos el carácter no estacionario del ruido variando las secuencias del ruido (semillas) para cada amplitud de ruido superpuesto, manteniendo sus propiedades estadísticas. Nuestros resultados numéricos indican que el ruido para este forzamiento estocástico no estacionario se vuelve menos contundente conforme aumenta la complejidad de las señales subumbrales.

*Descriptores:* Resonancia estocástica; sistema excitable.

PACS: 05.45.-a; 82.40.Bj; 87.19.lc

### 1. Introduction

Since the 1980s, enormous interest has been generated by the studies involving the response of excitable dynamical systems when subjected to stochastic fluctuations. One of the most relevant results obtained was the identification of Periodic Stochastic Resonance (PSR) [1, 2], a phenomenon by means of which a subthreshold periodic signal is amplified with a high degree of fidelity and synchrony for an optimal amplitude of the superimposed noise. Another manifestation of this SR phenomenon was detected, when instead of the subthreshold periodic signal, an aperiodic subthreshold signal was employed. In this case, it was found that for an optimal level of noise, response of the excitable system tends to synchronize with the subthreshold aperiodic signal, or in other words, an augmented degree of information transfer is observed. This phenomenon, called Aperiodic Stochastic Resonance (ASR), has also been reported in the literature [3–5].

Subsequently, it was realized [6] that the resonance behavior persists even in the absence of the subthreshold signal, implying that a purely stochastic signal can also induce enhanced regularity in excitable systems. This Coherence Resonance (CR) [6–8] effect is yet another example of the constructive role of noise in excitable systems. The review article written by Gammaitoni *et al.* [9] is a useful dossier that documents the advances achieved in the field of SR and its numerous extensions both from a theoretical and an experimental perspective.

It is presumed that since stochastic resonance is a generic phenomena it would appear whenever noise is suitably introduced in nonlinear systems. In the present work, we explore for cases in which it could be difficult to confirm the inception of this stochastic resonance effect. In particular, we consider the situation where the superimposed stochastic fluctuations are drifting with time due to the finite length of the noise sequence. It is well known that prevalent noise in real systems, particularly biological systems, is non-stationary. Consequently, it is of relevance, under these conditions, to verify the robustness of noise invoked resonances. This involves calculating the resonance curves employing different sequences of the noise signal at each noise amplitude. Diverse scenarios, both in the absence and the presence of subthreshold signals (periodic and aperiodic) are analyzed.

### 2. Model and method

The excitable FitzHugh-Nagumo system is described by the following set of coupled nonlinear equations:

$$\begin{aligned}\epsilon \frac{dx}{dt} &= x - \frac{x^3}{3} - y, \\ \frac{dy}{dt} &= x + a + S, \end{aligned} \quad (1)$$

where  $\epsilon = 0.01$ ,  $a$  is the bifurcation parameter and  $S$  represents the externally superimposed (stochastic and subthreshold) perturbations. For  $a > 1$ , the autonomous model dynamics exhibits an excitable fixed point behavior whereas for  $a < 1$ , a stable limit cycle behavior is found.  $a = 1$  corre-

sponds to the bifurcation point where the system undergoes a Hopf bifurcation. The integration of differential equations (1) was performed using a second order Stochastic Runge-Kutta integrator [10] with a step size of  $h = 10^{-3}$ .

For the case of PSR and CR, the regularity observed in the system dynamics was quantified using the normalized variance

$$V_n = \frac{\sqrt{\text{var}(t_p)}}{\langle t_p \rangle},$$

where  $t_p$  is the time elapsed between two successive spikes. The lower the value of  $V_n$ , the higher the degree of coherence induced in the system. Meanwhile, to compute the resonance curves for the situations involving complex subthreshold signals, normalized cross correlation (Power Norm) was utilized. This Power Norm is defined as

$$P_n = \left| \frac{\langle (x_1 - \langle x_1 \rangle)(x_2 - \langle x_2 \rangle)_t \rangle}{\langle x_1 \rangle_t \langle x_2 \rangle_t} \right|,$$

where  $x_1$  corresponds to the time series of the subthreshold signal and  $x_2$  is the time series associated with the response signal [ $y$  in Eqs. (1)].  $\langle \cdot \rangle_t$  denotes the time average.  $P_n$  gives us the coincidence measure (fidelity/synchrony) between the subthreshold signal and the system response. Larger values of  $P_n$  reflect higher values of information transfer between the input (complex subthreshold signal) and the output (response of the excitable system).

The superimposed noise for all the numerical computations presented below is a Gaussian white noise  $\xi$  with zero average ( $\langle \xi(t) \rangle = 0$ ), unit variance and delta type correlations ( $\langle \xi(t)\xi(t') \rangle = \delta(t - t')$ ). To ensure reasonable statistics, around 10,000 peaks (corresponding to 10,000,000 data points) from the system (FN model) response are considered at each noise amplitude. This information is subsequently utilized for the calculation of  $V_n$  (CR and PSR) or  $P_n$  (ASR) at that noise amplitude.

### 3. Results

The curves of Fig. 1, corresponding to the CR phenomenon, were generated by adding noise to the system  $S = D\xi$  in Eqs. (1), where  $D$  is the magnitude of the superimposed white noise.

The white curve of Fig. 1 corresponds to the situation where the same noise sequence was used repeatedly (“same seed”) for different values of the noise strength. The black curve was generated using distinct noise sequences (“different seed”) each time  $V_n$  was calculated. As expected, the resonance curve maintains its unimodal profile for the scenario involving different noise sequences.

The resonance curves in Fig. 2 were obtained by adding a subthreshold periodic component  $P$  to the noise fluctuations, *i.e.*  $S = P + D\xi$ , corresponding to the PSR phenomenon. This periodic pulse train, shown in the inset of the panel, has a period of 2 time units, an amplitude of 0.24 units, and a

pulse width of one time unit. Similar to the CR curves, the resonance curves observed for the PSR effect seems to be insensitive to the particular details of the superimposed noise sequences.

In the third phase of the present work, the robustness of the ASR phenomenon was analyzed. An aperiodic pulse train whose inter-pulse interval had a stochastic distribution (upper trace in the time series plots from Fig. 3) was constructed and subsequently utilized as the subthreshold signal. In the left panel of Fig. 3, the curves corresponding to the Power Norm ( $P_n$ ) are presented. The upper curve in the left panel was calculated using the same noise sequence. It exhibits the standard unimodal ASR curve. The three time series for this

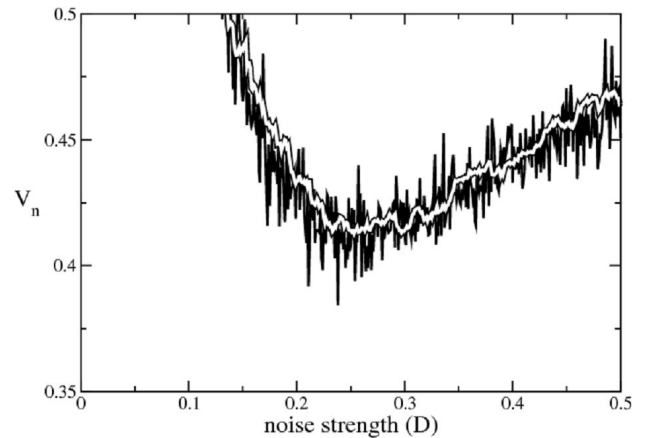


FIGURE 1. Plot associated with the Coherence Resonance phenomenon. The white curve was generated using the same noise sequence for each value of the noise strength ( $D$ ). The black curve involved employing different noise sequences for each value of  $D$ . The model parameters for Eq. (1) were fixed at  $\epsilon = 0.01$  and  $a = 1.25$ .

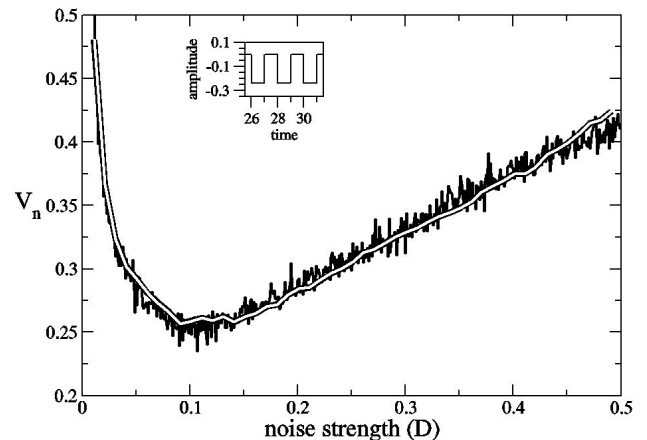


FIGURE 2. Plots associated with the PSR phenomenon. The white curve was generated using the same noise sequence for each value of the noise strength ( $D$ ). The black curve involved employing different noise sequences for each value of  $D$ . Moreover, in the inset of the panel, the subthreshold periodic signal ( $P$ ) is presented. The model parameters for Eq. (1) were fixed at  $\epsilon = 0.01$  and  $a = 1.25$ .

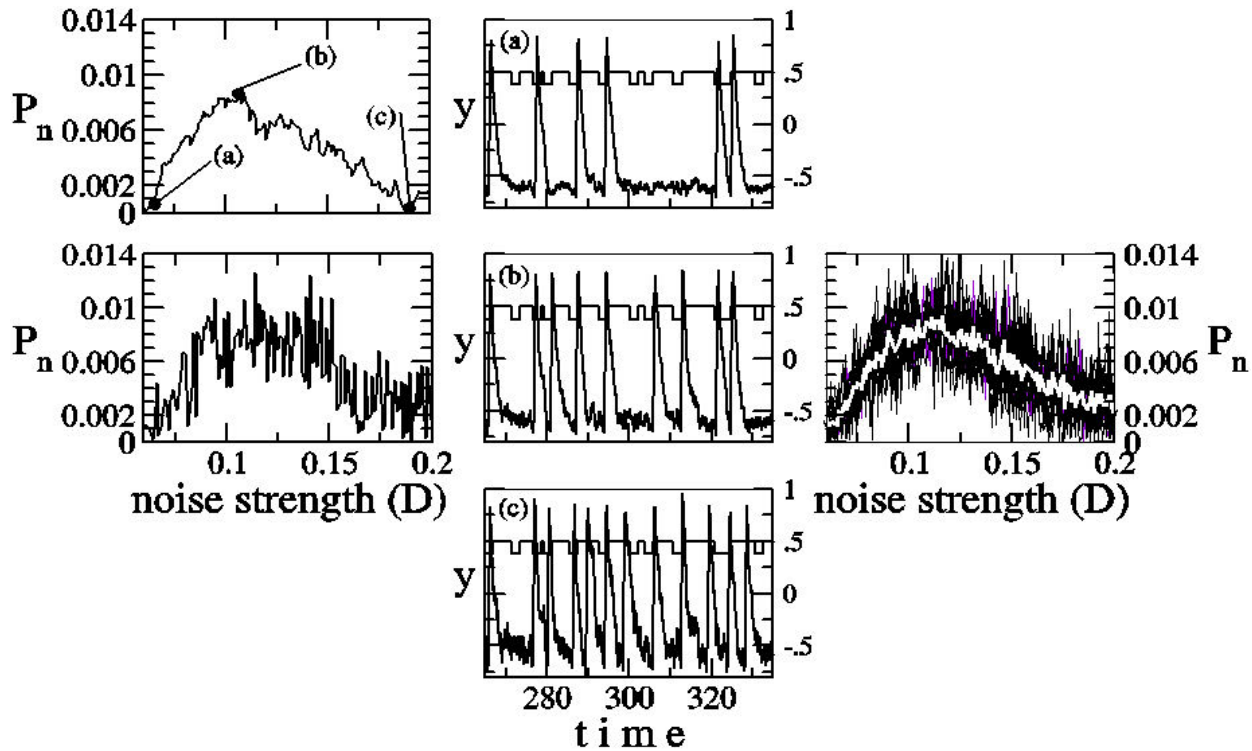


FIGURE 3. Plots corresponding to the ASR phenomenon using an aperiodic pulse train as the subthreshold signal. Left panel: The upper  $P_n$  curve in the left panel was generated using the same noise sequence for each value of the noise strength ( $D$ ). The lower curve in the left panel involved employing different noise sequences for each value of  $D$ . Middle panel: Three time series plots of the model variable  $y$  when subjected to the same noise sequence repeatedly. The noise amplitudes correspond to the points (a), (b) and (c) indicated in the upper left panel. Also superimposed (different scale) is the subthreshold signal constructed for the ASR effect. Right panel: Fifteen superimposed  $P_n$  curves where a different noise sequence was chosen for each noise strength. The average curve, represented by a white line, reveals a unimodal profile. The model parameters values are identical to the ones presented in the previous figure captions.

set of numerical simulations, presented in the middle panels, correspond to extremal points (a), (b), and (c). They depict enhanced information transfer between the input (complex subthreshold signal) and the output (model response) for an optimal amplitude (b) of noise. In comparison, the lower curve of the left panel shows the  $P_n$  values when one uses different noise sequences for each amplitude of noise. The high amplitude fluctuations in  $P_n$  values make it hard to reliably detect the presence of an underlying resonance in the individual curve computed using different noise seeds. Consequently, it is difficult to locate the optimum amplitude of the superimposed noise which provokes maximal correspondence between the subthreshold signal and the system response. To rectify this anomaly, we needed to perform multiple numerical calculations and superimpose the generated resonance curves. As shown in graph of the right panel, the average Power Norm ( $P_n$ ) (white line) from repeated numerical experiments does reveal a unimodal resonance curve for different noise sequences.

In the final set of numerical experiments, a more complex subthreshold signal was used. This aperiodic series was constructed using a stochastic distribution of the pulse amplitude including both negative and positive signs. Moreover, the inter-pulse interval is stochastically distributed. In the left panel of Fig. 4, the computed Power Norm curves using this aperiodic subthreshold sequence are presented. In the upper plot of the left panel, the  $P_n$  curve is calculated using the same noise sequence. The lower plot in the left panel corresponds to the scenario in which a different noise sequence is employed for each value of the noise amplitude. It is evident that in both the curves the ASR phenomenon is, at best, unclear. Therefore, the augmented complexity of the employed subthreshold signal makes it harder to decipher the noise provoked resonance.

Once again, we needed to compute multiple resonance curves for both scenarios (same seed and different seeds) to reveal the underlying resonance behavior. As shown in the upper and lower graphs of the right panel in Fig. 4, the computed average  $P_n$  curves do exhibit a unimodal profile by virtue of the ASR phenomenon.

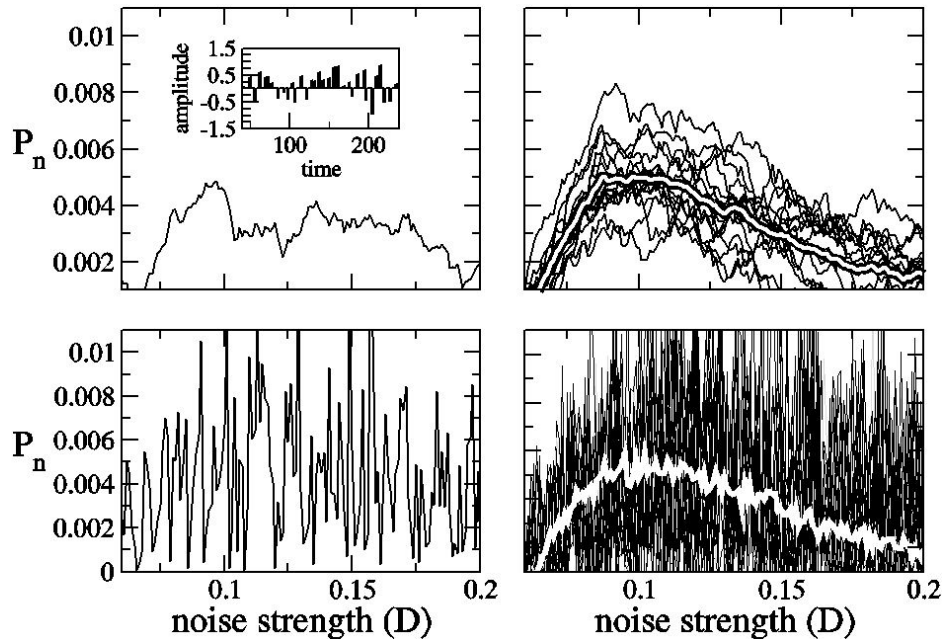


FIGURE 4. The upper  $P_n$  curve in the left panel was generated using the same noise sequence for each value of the noise strength ( $D$ ). The lower curve in the left panel involved employing different noise sequences for each value of  $D$ . Also presented in the inset of the upper plot is the subthreshold aperiodic signal used for this set of ASR calculations. The upper curves in the right panel represent fifteen superimposed  $P_n$  curves where the noise sequence remained unchanged for different noise strengths. The average curve, represented by a white line, reveals a unimodal profile. The lower curves in the right panel correspond to fifteen superimposed  $P_n$  curves where noise sequence was varied for different noise strengths. Yet again, the average curve, represented by a white line, reveals a unimodal profile. The model parameters values are identical to the ones presented in the previous figure captions.

#### 4. Remarks

- 1) For the simple cases of CR and PSR, it is possible to confirm the persistence of the noise induced resonances. The observed resonance behavior, as expected, is insensitive to whether the superimposed noisy perturbations emanates from the same seed or from different seeds for each value of the superimposed noise.
- 2) The invoked resonances become less conclusive as the complexity of the subthreshold signals is augmented (ASR). This consequently leads to enhanced uncertainty in the location of the optimal noise amplitude for which maximum information transfer is achieved. This result is of possible relevance to systems where the prevalent noise is non-stationary as it would lead to the smearing of the ASR effect.
- 3) One can unmask the ASR phenomenon by superimposing numerous noise provoked curves and calculat-

ing their average. This averaging technique [3, 12, 13] seems to be appropriate in revealing the noise induced resonances in the presence of complex subthreshold signals and non-stationary noise.

- 4) In real systems, since the autonomous dynamics vary as well, it is quite probable that the ASR effect might not be recovered using this average technique for the following reason: The drift of the system behavior could shift the location of the bifurcation point and effectively move the set-point. This relocation of the bifurcation and the set-points would render the averaging technique ineffective making it impossible to reveal the smeared ASR phenomena.

#### Acknowledgments

We wish to acknowledge the financial support received from CONACyT via projects 48354-F and 59329.

1. R. Benzi, A. Sutera, and A. Vulpiani, *J. Phys. A* **14** (1981) 453.
2. G. Nicolis, and C. Nicolis, *Tellus* **33** (1981) 225; C. Nicolis and C. Nicolis, *Tellus* **34** (1982) 1.
3. J.J.Collins, C.C. Chow, and T.T. Imhoff, *Phys. Rev. E* **52** (1995)

R3321.

4. C. Eichwald and J. Walleczek, *Phys. Rev. E* **55** (1997) R6315.
5. P. Parmananda, Gerardo J. Escalera Santos, M. Rivera, and K. Showalter, *Phys. Rev. E* **71** (2005) 031110.

6. S. Arkady Pikovsky and Jürgen Kurths, *Phys. Rev. Lett.* **78** (1997) 775.
7. G. Giacomelli, M. Giudici, S. Balle, and J. R. Tredicce, *Phys. Rev. Lett.* **84** (2000) 3298.
8. G.J. Escalera Santos, M. Rivera, M. Eiswirth, and P. Parmananda, *Phys. Rev. E* **70** (2004) 021103.
9. L. Gammaitoni, P. Hanggi, P. Jung, and F. Marchesoni, *Rev. Mod. Phys.* **70** (1998) 223.
10. H. S. Greenside and E. Helfand, *Bell Syst. Tech. J.* **60** (1981) 1927.
11. J. Escalona, Gerardo J. Escalera Santos, and P. Parmananda, *Phys. Rev. E* **76** (2007) 016213.
12. C. Heneghan *et al.*, *Phys. Rev. E* **54** (1996) R2228.
13. A. Capurro, K. Pakdaman, T. Nomura, and S. Sato, *Phys. Rev. E* **58** (1998) 4820.